Numerical solution for two-dimensional flow under sluice gates using the natural element method

Farhang Daneshmand, S.A. Samad Javanmard, Tahereh Liaghat, Mohammad Mohsen Moshksar, and Jan F. Adamowski

Abstract: Fluid loads on a variety of hydraulic structures and the free surface profile of the flow are important for design purposes. This is a difficult task because the governing equations have nonlinear boundary conditions. The main objective of this paper is to develop a procedure based on the natural element method (NEM) for computation of free surface profiles, velocity and pressure distributions, and flow rates for a two-dimensional gravity fluid flow under sluice gates. Natural element method is a numerical technique in the field of computational mechanics and can be considered as a meshless method. In this analysis, the fluid was assumed to be inviscid and incompressible. The results obtained in the paper were confirmed via a hydraulic model test. Calculation results indicate a good agreement with previous flow solutions for the water surface profiles and pressure distributions throughout the flow domain and on the gate.

Key words: free surface flow, meshless methods, meshfree methods, natural element method, sluice gate, hydraulic structures.

Résumé : Les charges de fluides sur les structures hydrauliques et le profil de la surface libre de l'écoulement sont importants aux fins de conception. Cette conception est une tâche difficile puisque les équations principales présentent des conditions limites non linéaires. Cet article a comme objectif principal de développer une procédure basée sur la méthode des éléments naturels (NEM) pour calculer les profils de la surface libre, les distributions de vitesse et de pression ainsi que les débits pour un écoulement gravitaire bidimensionnel sous les panneaux de vannes. La NEM est une technique numérique dans le domaine de la mécanique computationnelle et peut être considérée comme étant une méthode sans maillage. Dans la présente analyse, le fluide était présumé être exempt de viscosité et incompressible. Les résultats obtenus ont été vérifiés par un essai du modèle hydraulique. Les résultats des calculs montrent une bonne corrélation entre les solutions d'écoulement antérieures pour les profils de surface de l'eau et les distributions de pression dans tout l'écoulement et sur la vanne.

Mots-clés : écoulement de surface libre, méthodes sans maillage, méthode par éléments naturels, panneaux de vanne, structures hydrauliques.

[Traduit par la Rédaction]

Introduction

The analysis of two-dimensional gravity affected flows involving a free surface is an important area of research in hydraulic engineering. Examples include flows over hydraulic structures such as spillways, weirs and various types of gates. Flow characteristics of interest may include the velocity and pressure distributions and the free surface profile. In all these problems, when steady state prevails, the flow is governed by an elliptic partial differential equation. On the known part of the boundary, one boundary condition is specified while on the free surface of the flow two boundary conditions should be satisfied. The determination of the free surface location as a part of the solution involves the solution of an intrinsically nonlinear problem.

One of the major achievements in classical hydrodynamics was the use of complex analysis and conformal transformations in solving free surface flows as presented by Larock (1970). Such analytical solutions are limited in number be-

F. Daneshmand[1,2] and S.A.S. Javanmard. Faculty of Mechanical Engineering, Shiraz University, Shiraz, Iran.
T. Liaghat. Dorj-Danesh Company, Shiraz 71348-51154, Iran.
M.M. Moshksar. Department of Material Science and Engineering, School of Engineering, Shiraz University, Shiraz 71348-51154, Iran.
J.F. Adamowski. Department of Bioresource Engineering, Faculty of Agricultural and Environmental Sciences, McGill University, 21111 Lakeshore Road, Ste. Anne de Bellevue, QC H9X 3V9, Canada.

[1]Corresponding author (e-mail: farhang.daneshmand@mcgill.ca).
[2]Present address: Department of Mechanical Engineering, McGill University, Montreal, QC H3A 2K6, Canada.

cause of the difficulty in satisfying the nonlinear condition of constant pressure along the free surface.

Among the numerical methods, the finite element method (FEM) has gained more popularity in solving the free surface problem. A lot of research in this area appears in the literature, including the work of Chan et al. (1973), Isaacs (1977), and Sankaranarayanan and Rao (1996). An important contribution to the finite element analysis of potential flows having free surfaces was provided by Daneshmand et al. (1999, 2000) and Daneshmand and Kazemzadeh Parsi (2004), all of whom conducted research to find the free surface shapes of the flow under radial gates. A combination of a variable domain and a fixed domain finite element method was used by these authors and it was shown that the iteration procedure converges rapidly.

Although the finite element method is robust and has been thoroughly developed, it necessitates regeneration of the meshes in solving free surface problems. This is frequently done by the modeler, and is considered to be one of the most time-consuming tasks in finite element analysis.

To overcome the difficulty associated with remeshing, the past decade has seen a tremendous surge in the development of a family of Galerkin and collocation-based numerical methods known as meshless methods. For example, some of the most widely used methods include the element-free Galerkin method (Belytschko et al. 1994), the reproducing kernel particle method (Liu et al. 1995), and the natural neighbor Galerkin methods, or natural element methods (NEM) (Sukumar and Moran 1999). The essential characteristic of the meshless methods is that there is no need for a highly structured mesh as required in the finite element methods.

The natural element method (NEM) is a Galerkin-based method that is built upon the principle of natural neighbor interpolation. This interpolation scheme has several very useful properties, such as its strictly interpolating character, ability to exactly interpolate piece-wise linear boundary conditions, and a well-defined and robust approximation with no user-defined parameter on non-uniform grids. The aim of this paper is to present a numerical procedure based on natural element discretization that treats the fluid flow through a sluice gate with a free surface. Despite some progress in solving gravity driven free surface flows through the use of the various numerical methods, solving the problem by using NEM has not been investigated to date. In the present study, the free surface profile, velocity and pressure distributions and the flow rate per unit width Q are calculated for a known Bernoulli constant, B, using the natural element method. Results for pressure distribution are compared with measured values obtained by conducting a hydraulic model test.

Statement of the problem and formulation

Figure 1 shows a typical two-dimensional steady flow under a sluice gate. The flow is assumed to be steady, two-dimensional, incompressible, and irrotational. The geometry of the gate, including the gate opening, b, the elevation above datum of the channel bed at every point, y, and the Bernoulli constant, B, are known. It should be noted that B and y are both measured from the same datum. Far upstream

and far downstream, where the depths are d_1 and d_2, respectively, the flow is assumed to be uniform and it is taken normal to the boundaries. In natural element analysis, these assumptions are used as boundary conditions in sections AF and DE. In the solved problems, satisfactory results were obtained with these sections located at $x = \pm 2B$ from the gate. The free surface profiles AS and CD must be found as part of the solution. Since the flow is assumed to be irrotational, it is governed by the Laplace equation:

[1] $$\frac{\partial^2 \psi}{\partial x^2} + \frac{\partial^2 \psi}{\partial y^2} = 0$$

where ψ is the stream function. Both the fixed boundaries and the free surface are streamlines; therefore ψ is taken to be a constant, i.e.

[2] $\psi = 0$ on the lower boundary

$\psi = Q$ on the free surface and on the sluice gate

where Q is the flow rate per unit width. On the free surface the dynamic boundary condition requires

[3] $$\frac{v^2}{2g} + y = B, \quad p = 0$$

where v is the velocity; g is the acceleration due to gravity; y is the free surface elevation measured from an arbitrary datum; B is the Bernoulli constant; and p is the pressure. Since

[4] $$v = \frac{\partial \psi}{\partial n}$$

where n is the unit normal from the free surface; eq. [3] becomes

[5] $$\frac{1}{2g}\left(\frac{\partial \psi}{\partial n}\right)^2 + y = B \text{ on a free surface}$$

Either the flow rate, Q, or the Bernoulli constant, B, are known; the other is required as part of the solution.

For the purposes of the numerical solution the inflow and outflow streams are cut at right angles to the primary velocity. On the cut portions the boundary condition

[6] $$\frac{\partial \psi}{\partial n} = 0$$

is applied, which means that there is no velocity normal to the main flow.

For problems with a known flow rate Q, the free surface profile is assumed and the problem is solved from eqs. [1], [2], and [6]. The constant, B, of eq. [3] is then calculated for the free surface nodes. If B is the same for all free surface points, the problem is solved. Otherwise, the assumed free surface is adjusted, iteratively, in order that B becomes constant at all points.

A similar procedure can be developed for problems with a given Bernoulli constant B. The problem is solved first by assuming the location of the free surface and applying the free surface conditions, eq. [5]. The flow rate, Q or ψ, of eq. [2] is part of the solution. If Q is a constant for all free surface points, the problem is solved; otherwise, an iteration scheme must be used to adjust the free surface elevation.

Fig. 1. Definition sketch of a vertical sluice gate.

Fig. 2. Definition of the natural neighbor coordinates for the determination of interpolation functions of point x based on NEM.

Since B = constant is considered in this paper, only the method for replacing the kinematics free surface condition is presented here (Cheng et al. 1981).

The natural element method

Natural element method is based on an interpolation plan called natural neighbor interpolation, which is frequently used for unstructured interpolation in geophysics (Watson

1981). This interpolation scheme is, in turn, based on the concepts of a Voronoi diagram and Delaunay triangulations (Sukumar et al. 1998).

A Delaunay triangulation is the unique triangulation for a given set of points that satisfies the empty circumcircle criterion. This means that the circumcircle of each triangle contains no other point than the three points that form the triangle. A first-order Voronoi diagram for a set of nodes $N = \{n_1, n_2, ..., n_m\} \in R^2$ is a subdivision of the space in regions T_I such that any point in T_I is closer to the node n_I, to which this region is associated, than to any other in N. Formally

$$[7] \quad T_I = \left\{ x \in R^2 : d(x, n_I) < d(x, n_J) \quad \forall \quad J \neq I \right\}$$

where $d(.,.)$ represents Euclidean distance. Two nodes whose associated Voronoi cells share an edge are called natural neighbors.

The natural neighbor interpolation scheme is based on the definition of the second order Voronoi tessellation. A cell T_{IJ} in the second-order tessellation is the locus of points that have node I as the closest node and the node J as the second closest node

$$[8] \quad T_{IJ} = \left\{ x \in R^2 : d(x, n_I) < d(x, n_J) < d(x, n_K) \quad \forall \quad K \neq I, J \right\}$$

If a new point x is introduced in the initial set N and the new tessellation is built, the natural neighbor coordinates of the point x with respect to one of its neighbors I is defined as the ratio of the area of T_I that has been transferred to T_x to the total area of T_{xI} that is shown in Fig. 2 (Watson 1994). Using $k(x)$ and $k_I(x)$ as Lebesgue measures (length in $\mathbf{R}^2$) (Sukumar et al. 1998) of T_x and T_{xI}, the natural neighbor coordinate of x with respect to the node I can be written as:

$$[9] \quad \varphi_I(x) = \frac{k_I(x)}{k(x)}$$

and with respect to Fig. 2 as:

$$[10] \quad \varphi_1 = \frac{A_{aef}}{A_{abcde}}$$

The other interpolation functions are presented in Table 1 and are compared with the interpolation functions obtained from FEM (Fig. 3).

From this definition, the unknown parameter field $u(x) : \Omega \subset R^2 \to R^2$ is approximated in the form

[11] $$u^h(x) = \sum_{I=1}^{n} \varphi_I(x) \ u_I$$

where u_I is the vector of nodal parameters of the n natural neighbors of the point x. The NEM formulated in this way has some remarkable properties in the context of meshless methods (Sukumar et al. 1998).

Using eqs. [9] and [10], it is clear that

[12] $$\varphi_i(x_j) = \delta_{ij}$$

and, consequently, the nodal parameters u_I are the nodal displacement. This allows us to impose nodal prescribed values by directly substituting them in the Galerkin procedure.

The linear consistency of the interpolant is derived after the local coordinate property

[13] $$x = \sum_{I=1}^{n} \varphi_I(x) x_J$$

in conjunction with the partition of unity property. This means that the natural neighbor interpolant can exactly reproduce a linear or constant displacement field. In the two-dimensional case, the approximation properties of the NEM interpolant depend on the relative node distribution. If a point x has only three natural neighbors, the interpolation obtained is equivalent to barycentric coordinates, or constant strain finite element interpolation functions. Bilinear interpolation is obtained over the rectangle if the point has four natural neighbors in a regular grid.

Discretization of the natural element method

The natural element solution of the ideal fluid flow (inviscid and incompressible flow) problem is considered in this section. The two-dimensional potential flow (irrotational flow) can be formulated in terms of a stream function (ψ). In terms of stream function, the governing equation is the Laplace equation where the flow velocities v_x and v_y are

[14] $$v_x = \psi_{,y} \quad v_y = -\psi_{,x}$$

The Dirichlet and Neumann boundary conditions are shown in Fig. 1 by C_1 and C_2, respectively.

To use the natural element method using the Galerkin approach, the problem domain S is first divided into elements, and a suitable interpolation model is then assumed for $\psi^{(e)}$ as

[15] $$\psi^{(e)}(x, y) = \sum_{i=1}^{m} \varphi_i(x, y)\psi_i^{(e)}$$

where $\varphi_i(x, y)$ is the natural element interpolation function and m is the number of neighborhoods of point (x, y). In the Galerkin method, the test functions and the trial functions are taken from the same set of functions. Choosing φ_i according to the Galerkin approach, the discretized form of eq. [1] becomes

[16] $$\iint_{S^{(e)}} \varphi_i \left[\frac{\partial^2 \psi^{(e)}}{\partial x^2} + \frac{\partial^2 \psi^{(e)}}{\partial y^2} \right] dS = 0, \quad i = 1, 2, ..., m$$

Using the integration by-parts, this equation can be re-written as

[17] $$\iint_{S^{(e)}} \varphi_i \left(\frac{\partial \varphi_i}{\partial x} \frac{\partial \psi^{(e)}}{\partial x} + \frac{\partial \varphi_i}{\partial y} \frac{\partial \psi^{(e)}}{\partial y} \right) dS$$
$$- \int_{C^{(e)}} \varphi_i \left(\frac{\partial \psi^{(e)}}{\partial x} n_x + \frac{\partial \psi^{(e)}}{\partial y} n_y \right) dC = 0$$

Applying the Dirichlet and Neumann boundary conditions given on $C_1^{(e)}$ and $C_2^{(e)}$

[18] $$\int_{C^{(e)}} \varphi_i \left(\frac{\partial \psi^{(e)}}{\partial x} n_x + \frac{\partial \psi^{(e)}}{\partial y} n_y \right) dC = \int_{C_2^{(e)}} V_0 \varphi_i dC_2$$

By using eqs. [15] and [18], eq. [17] can be expressed in matrix form as:

[19] $$\mathbf{K}^{(e)} \psi^{(e)} = \mathbf{P}^{(e)}$$

where

[20] $$\mathbf{K}^{(e)} = \iint_{S^{(e)}} \mathbf{B}^T \mathbf{B} dS$$

[21] $$\mathbf{P}^{(e)} = -\int_{C_2^{(e)}} V_0 \mathbf{N}^T dC_2$$

[22] $$\mathbf{B} = \begin{bmatrix} \dfrac{\partial \varphi_1}{\partial x} & \dfrac{\partial \varphi_2}{\partial x} & \cdots & \dfrac{\partial \varphi_m}{\partial x} \\ \dfrac{\partial \varphi_1}{\partial y} & \dfrac{\partial \varphi_2}{\partial y} & \cdots & \dfrac{\partial \varphi_m}{\partial y} \end{bmatrix}$$

[23] $$\mathbf{N}^T = \begin{bmatrix} \varphi_1 & \varphi_2 & \cdots & \varphi_m \end{bmatrix}$$

Using the above element matrices and the assembling procedure, the following system of equations can be obtained

[24] $$\mathbf{K}\psi = \mathbf{P}$$

where $\mathbf{K}$ is the total system matrix for the problem, ψ is the vector including the unknown nodal values of the stream function, and $\mathbf{P}$ is the total load vector.

The system matrix calculation for two different methods, FEM and NEM, is described in Appendix A.

Free surface correction

The geometry of a vertical sluice gate is shown in Fig. 1. If the Bernoulli constant is known, the iterative scheme for adjusting the free surface locations can be described as follows. Introducing $\bar{v}$ as the average velocity at a vertical cross section, the flow rate can be expressed as

Table 1. Interpolation functions in FEM and NEM.

Interpolation function	φ_1	φ_2	φ_3	φ_4	φ_5
FEM	0	A_{x45}/A_{245}	0	A_{x25}/A_{245}	A_{x24}/A_{245}
NEM	A_{aef}/A_{abcde}	A_{abhgf}/A_{abcde}	A_{bch}/A_{abcde}	A_{cdgh}/A_{abcde}	A_{defg}/A_{abcde}

Fig. 3. Determination interpolation functions of point *x* based on FEM.
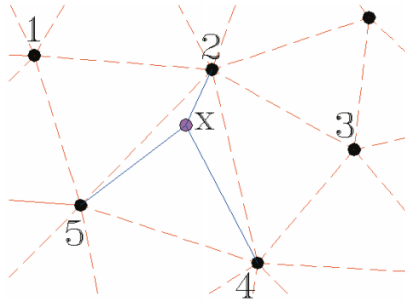
Fig. 4. Mesh generated using α-shape theory.
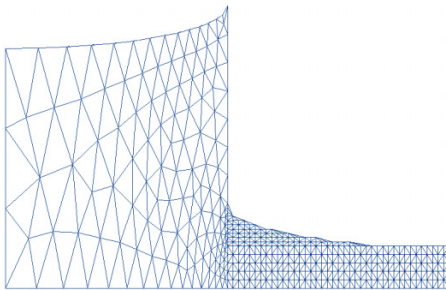
Fig. 5. Algorithm for finding the free surface.
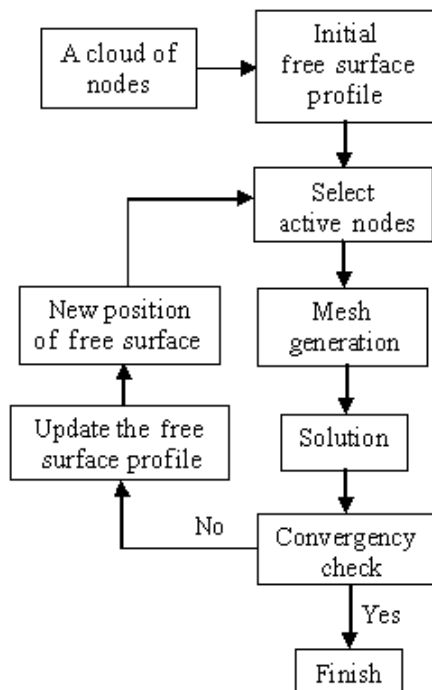
Fig. 6. Comparison between BIEM (Cheng et al. 1981) and NEM (Example 1).
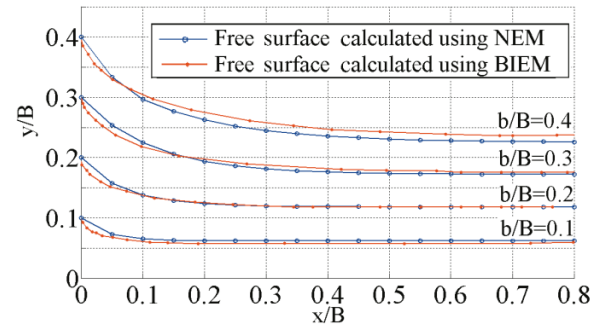
$$[25] \quad Q = \bar{v}y$$

where *y* is the free surface elevation measured from an arbitrary datum. For free surface adjustment, it is assumed that $\bar{v}$ is the free surface velocity, *v*. The problem is solved by replacing the kinematic free surface condition eq. [2] with the dynamic free surface condition eq. [5]. After solving the governing equation using the boundary conditions and NEM, the solution yields different values of the stream function at each of the free surface nodes. A temporarily "correct" flow rate, Q^{k+1}, is needed for performing the free surface adjustment. The calculated value of the stream function ψ_c^k (at point *C*) can be considered a good estimation for Q^{k+1}

$$[26] \quad Q^{k+1} = \psi_c^k$$

By taking $\Delta y_i = y_i^{k+1} - y_i^k$; $\Delta Q_i = Q^{k+1} - \psi_i^k$ and substituting eq. [25] into eq. [5], the following equation is obtained

$$[27] \quad \frac{\left(\psi_i^k + \Delta Q_i\right)^2}{2g\left(y_i^k + \Delta y_i\right)^2} + y_i^k + \Delta y_i = B$$

After linearizing and solving for Δy_i

$$[28] \quad \Delta y_i = -\frac{\psi_i^k}{g\left(y_i^k\right)^2}\left[\Delta Q_i \bigg/ \left(1 - \frac{(\psi_i^k)^2}{g(y_i^k)^3}\right)\right]$$

For large gate openings, however, the Froude number (Q^2/gy^3) for portions of the downstream profile is not much larger than unity. In those cases Δy_i of eq. [18] tends to be too large. A more conservative, yet stable, scheme is used whenever the foregoing is observed
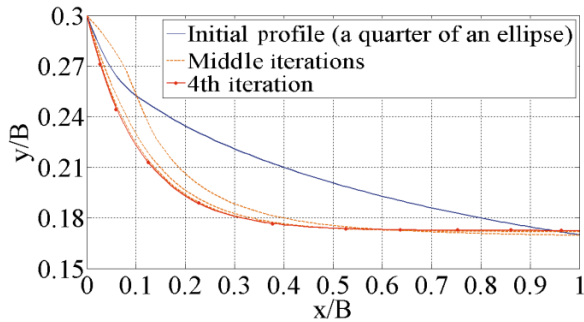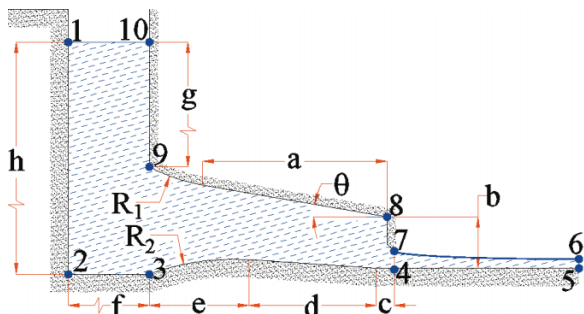
$$[29] \quad \Delta y_i = \frac{\Delta Q_i}{\psi_i^k}y_i^k$$

Thus, eq. [28] or eq. [29] lead to a new location of the free surface.

Table 2. Results from NEM for $\varepsilon = 0.001$ (Example 1).

	b/B			
	0.1	0.2	0.3	0.4
Numer of nodes (in first iteration)	109	155	108	158
Number of elements (in first iteration)	121	217	147	233
Number of iterations	3	2	3	4
Calculated ψ on free surface (m³ s⁻¹ m⁻¹)	0.481	0.891	1.258	1.591

Fig. 7. Free surface profiles for $b/B = 0.3$ and $\varepsilon = 0.001$ (Example 1).
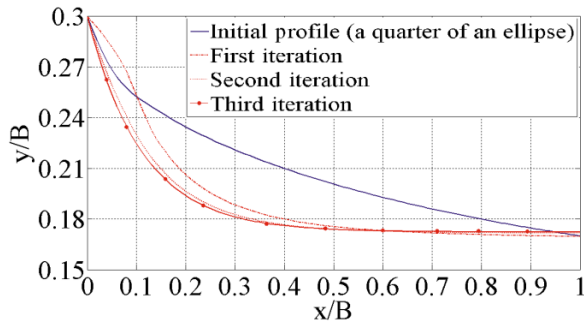
Fig. 8. Free surface profiles for $b/B = 0.3$ and $\varepsilon = 0.0001$ (Example 1).

Table 3. Shahryar Dam specifications (Example 2).

Parameter	Value (description)
Type	Double-arch concrete dam
Height (from the river bed)	135
Crest elevation	1045
Bottom outlet sill elevation	1004
Total storage (at normal water level)	700×10^6 m³
Normal water level (NWL)	1035
Maximum water level	1041

Note: All units are expressed in metres unless otherwise noted.

Table 4. Technical specifications (Example 2).

Parameter	Value	Parameter	Value
a	1	h_1	0.061
b	0.288	h_2	0.178
b_1	0.233	H_1	0.306
c	0.1	H_2	0.041
d	0.71	R	0.02
e	0.55	R_1	1
f	1.5	R_2	1.33
g	2.4	α	45°
h	3	Θ	10°

Note: All units are expressed in metres unless otherwise noted.

Fig. 9. Specification of Shahryar Dam (Example 2).

Fig. 10. Position of manometers on sluice gate (Example 2).

Computational scheme

In this paper, the amount of discharge, the free surface profile, and the pressure distribution in the channel along the fluid boundaries and on the gate, should be computed for a given total head. The computer implementation of this numerical procedure includes the following steps:

(1) A cloud of nodes in the initial problem domain is assumed.
(2) The initial trial free surface, a quarter of an ellipse, is assumed and the nodes under and on the assumed free surface profile are selected as the active nodes in the problem domain.
(3) Delaunay triangulation is used to create elements from the cloud of nodes.

Fig. 11. Position of manometers on channel wall (Example 2).
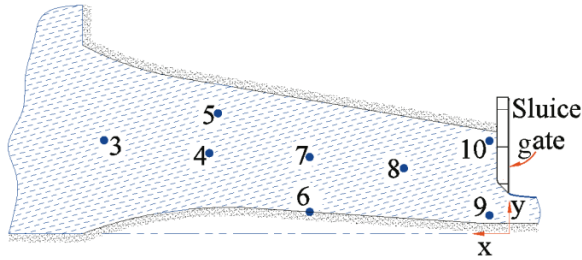
(4) The α-shape theory (Alfaro et al. 2006) is used to delete some elements generated outside the boundaries of the problem domain (Fig. 4). In this method, given a finite point set, a family of shapes can be derived from the Delaunay triangulation of the point set and a real parameter α controls the desired level of detail.

(5) The problem is solved using NEM by applying Dirichlet and Neumann boundary conditions as explained in the previous sections. The value of discharge (ψ) and velocity components (v_x, v_y) for all nodes are calculated as a function of the assumed free surface profile.

(6) The flow rate Q^{k+1} can then be calculated using the results obtained from step 5 and applying eq. [26]. The iteration process is continued until the maximum value of the convergence criterion defined as $|Q^{k+1} - \psi_i^k|/Q^{k+1}$ is less than a prescribed accuracy ε.

If the above convergence criterion from step 6 is satisfied, the last assumed free surface profile is chosen as the final free surface profile; otherwise, the displacement for each node on the free surface is calculated using eq. [28] or eq. [29]. The new free surface profile is defined by the new location of nodes and step 3 is repeated until desired accuracy is achieved. The nodes on the new free surface profile are selected as the active nodes for subsequent steps. The above algorithm is shown in Fig. 5.

When the accuracy calculated for each node on the free surface is less than the desired accuracy, the velocity and pressure distribution can be calculated for each node.

Application and discussion of results

To examine the applicability of the numerical scheme described in the previous sections, two different examples were considered. The example problems were selected such that the present results could be compared with published results obtained by numerical or physical modeling.

Example 1

Example 1 has been chosen to compare the results obtained by using the natural element method (NEM) presented in this paper with the results obtained by using the boundary integral element method (BIEM) (Cheng et al. 1981). Results presented by Montes (1997) for free surface profile calculations were very close to the results obtained by Cheng et al. (1981). The sluice gate geometry is shown in Fig. 1 with $B = 1$ (arbitrary length unit) and $b = 0.3$ (gate opening). The initial trial upstream and downstream free surface profile is fitted by a quarter of an ellipse with an arbitrary downstream depth of $y = 0.5b$. The computational prescribed accuracy is defined by ε.

In the first step, the model is considered for different values of $b/B = 0.1, 0.2, 0.3$ and 0.4 and $\varepsilon = 0.001$ for finding the free surface profile using NEM. The free surface adjustment scheme eq. [28] or eq. [29] is used to find the new free surface location. The results are shown in Fig. 6 and Table 2. It can be seen that the results obtained through the use of the procedure using NEM are in good agreement with those obtained from BIEM.

In the second step, the flow under the sluice gate is modeled for $b/B = 0.3$ and different values of $\varepsilon = 0.001$ and $\varepsilon = 0.0001$. The transition of the downstream profile is plotted in Figs. 7 and 8 via the use of NEM. It is observed that the free surface profile in NEM converged faster than in BIEM. This result was obtained by comparing the number of iterations of the two methods for specified accuracy. The convergence was obtained after six iterations on the free surface profile with $\varepsilon = 0.001$ using BIEM, whereas only three iterations were needed to achieve the same accuracy using NEM. It may also be noted that four iterations is sufficient to find the free surface profile with $\varepsilon = 0.0001$ using the natural element method.

Example 2

The two-dimensional flow through a conduit and under a sluice gate was considered in this second example. Figure 9 shows the definition sketch of the bottom-outlet sluice gate of Shahryar Dam. The Shahryar Dam is located on the Ghezel-Oezan River in Iran, near Miyaneh city. The dam specifications and geometric details of the problem are given in Tables 3 and 4, respectively. The value of head loss for this example was calculated in accordance with the traditional procedure given in Roberson and Clayton (1997) for the entrance loss (loss coefficient = 0.03) and Brno Technical University (1994) for the outlet loss due to sudden contraction, respectively. To ensure the validity of the results obtained in this example, a hydraulic model test (scale 1:15) based on Froude's law of similarity was also constructed (Shiraz University 2007). The hydraulic model test includes the entire water passage both upstream and downstream of the gate. The hydraulic model is constructed using plexiglass material to secure good flow visualization. For better visualization of the free surface profile, the downstream wall of the model is meshed by squares 5 cm × 5 cm. The test stand includes three centrifugal pumps, as well as main water storage and relevant channels to complete the closed loop circuit. For measuring pressure, some manometers are installed at different points in the channel and skin plate on the gate. The manometer locations are shown in Figs. 10 and 11. The unit of measured pressure is mH_2O. Water discharge was measured by using a rectangular weir placed downstream of the model, whereas the measured values are also checked and confirmed by using the area–velocity flow meter (Greyline AVFM-II). Its ultrasonic sensor was installed at the bottom of the downstream channel. Based on the speed of sound in water, the level is measured with an accuracy of ±0.25%. Flow velocity was also measured with an ultrasonic Doppler signal. The instrument measures velocity with an accuracy of ±0.2%.

The natural element method was used to solve the problem. The discretization was made finer in the vicinity of the gate to take care of the higher velocity gradients that exist in

Table 5. Comparison between numerical and experimental results (Example 2).

Manometer #	$p(mH_2O)$ (Model test)	$p(mH_2O)$ NEM	Error (%)	ψ (m³ s⁻¹ m⁻¹) NEM	v (m/s) NEM
1	2.133	2.245	4.98	0.283	2.678
2	2.175	2.235	2.67	0.299	0.787
3	2.203	2.187	0.70	0.137	0.530
4	2.204	2.214	0.49	0.133	0.755
5	2.080	2.088	0.41	0.230	0.754
6	2.363	2.393	1.25	0.001	0.853
7	2.191	2.220	1.30	0.148	0.846
8	2.187	2.248	2.70	0.154	0.936
9	2.037	2.148	5.15	0.058	2.488
10	2.165	2.204	1.77	0.291	0.307

Note: p is pressure; NEM is natural element method; ψ is the stream function; v is velocity.

Fig. 12. Free surface profile for gate opening 30% (Example 2).

Fig. 13. Velocity distribution contour for gate opening 30% per m/s (Example 2).
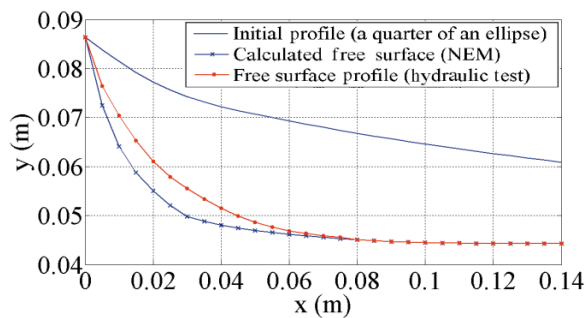
that region. The domain bounded by the surfaces 1–2–3–4–7–8–9–10 in Fig. 9 is fixed and the matrix corresponding to the elements in this region may be calculated only once. However, the flow region bounded by 4–5–6–7 is a variable domain, and the system matrix related to the elements in this region should be calculated in successive iterations while an adjustment of the free surface is made. The sluice gate is considered in a 30% opening position. To solve the problem, 438 nodes and 662 elements are used in the first iteration.

In this example, the convergence was obtained on the free surface profile with a prescribed accuracy of $\varepsilon = 0.001$. The computed discharge Q is 0.299 m³ s⁻¹ m⁻¹. The pressure values are given in Table 5 and compared with the pressure values measured in the hydraulic model test. The shape of the free surface obtained from the present study is also compared with the free surface profile from the hydraulic model test in Fig. 12. As can be seen from this figure, the free surface profile obtained from NEM is in good agreement with that obtained from the model test. It should also be noted from Table 5 that the maximum error in pressure values is 5.15%. The velocity distribution contour for gate opening 30% is also shown in Fig. 13.

Conclusions

In this paper, the application of the natural element method (NEM) to the solution of gravity-affected flow under a sluice gate was studied. In NEM, the whole interpolation is constructed with respect to the natural neighbor nodes and Voronoi tessellation of the given point. The use of the natural neighbor Galerkin method was shown to be very useful in simulating physical phenomena. It is an appropri-

ate new approach to predict the behavior of gravity-affected flow under a sluice gate with excellent accuracy. A rapid rate of convergence is always observed even with an initial guess that differs greatly from the true solution. Numerical results show good agreement of the proposed method by comparing it to experimental results and the results of the boundary integral element method. The present scheme can be used with confidence in calculating the hydraulic parameters needed in the design of such structures. In spite of the nonlinear nature of the problem, the presented scheme does not need an excessive number of iterations. The iteration procedure converges quite rapidly. Although only flow under sluice gates was considered in this research, the range of future applications of the model can be extended to other similar flows (e.g., flow through a slit, flows over hinged gates, spillway crests, and weirs).
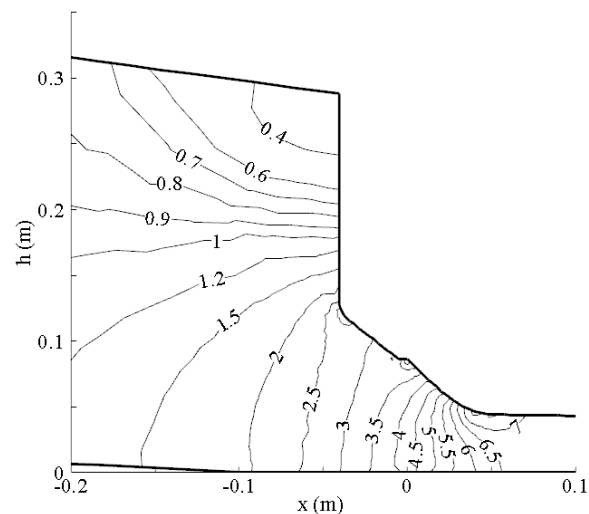
Acknowledgements

References

Alfaro, I., Bel, D., Cueto, E., Doblare, M., and Chinesta, F. 2006. Three-dimensional simulation of aluminum extrusion by the alpha-shape based natural element method. Computer Methods in Applied Mechanics and Engineering, **195**(33–36): 4269–4286. doi:10.1016/j.cma.2005.08.006.

Belytschko, T., Lu, Y.Y., and Gu, L. 1994. Element-free Galerkin methods. International Journal for Numerical Methods in Engineering, **37**(2): 229–256. doi:10.1002/nme.1620370205.

Brno Technical University. 1994. The bottom outlet Twin Gate, Marun. Water Management Research Institute, Czech Republic.

Chan, S.T.K., Larock, B.E., and Herrmann, L.R. 1973. Free surface ideal fluid flows by finite elements. Journal of the Hydraulics Division, **99**(No. HY6): 959–974.

Cheng, A.H.-D., Liggett, J.A., and Liu, P.L.-F. 1981. Boundary calculations of sluice and spillway flows. Journal of the Hydraulics Division, **107**(No. HY10): 1163–1178.

Daneshmand, F., and Kazemzadeh Parsi, M.J. 2004. A meshless method for free surface flow through sluice gates. 6th International Conference on Hydroinformatics, Singapur.

Daneshmand, F., Sharan, S.K., and Kadivar, M.H. 1999. Finite element analysis of double-free-surface flow through gates. Proceedings of the 17th Canadian Congress of Applied Mechanics, McMaster University, Hamilton, Ont. pp. 213–214.

Daneshmand, F., Sharan, S.K., and Kadivar, M.H. 2000. Finite element analysis of double-free surface flow through slit in dam. Journal of the Hydraulics Division, **126**(5): 515–522.

Issacs, L.T. 1977. Numerical solution for flow under sluice gates. Journal of the Hydraulics Division, **103**(5): 473–481.

Larock, B.E. 1970. A theory for free outflow beneath radial gates. Journal of Fluid Mechanics, Cambridge, U.K. **41**(4): 851–864. doi:10.1017/S0022112070000964.

Liu, W.K., Jun, S., and Zhang, Y.F. 1995. Reproducing kernel particle methods. International Journal for Numerical Methods in Fluids, **20**(8–9): 1081–1106. doi:10.1002/fld.1650200824.

Montes, J.S. 1997. Irrotational flow and real fluid effects under planer sluice gates. Journal of Hydraulic Engineering, **123**(3): 219–232. doi:10.1061/(ASCE)0733-9429(1997)123:3(219).

Roberson, J.A., and Clayton, T.C. 1997. Engineering fluid mechanics. 6th ed. Wiley, New York.

Sankaranarayanan, S., and Rao, H.S. 1996. Finite element analysis of free surface flow through gates. International Journal for Numerical Methods in Fluids, **22**(5): 375–392. doi:10.1002/(SICI)1097-0363(19960315)22:5<375::AID-FLD357>3.0.CO;2-O.

Shiraz University. 2007. Hydraulic model test of bottom outlet of Shahryar Dam. Report No. SHM-R-002-Shiraz-Iran.

Sukumar, N., and Moran, B. 1999. C^1 natural neighbor interpolant for partial differential equations. Numerical Methods for Partial Differential Equations, **15**(4): 417–447. doi:10.1002/(SICI)1098-2426(199907)15:4<417::AID-NUM2>3.0.CO;2-S.

Sukumar, N., Moran, B., and Belytschko, T. 1998. The natural element method in solid mechanics. International Journal for Numerical Methods in Engineering, **43**(5): 839–887. doi:10.1002/(SICI)1097-0207(19981115)43:5<839::AID-NME423>3.0.CO;2-R.

Watson, D. 1981. Computing the *n*-dimensional Delaunay tessellation with application to Voronoi polytopes. The Computer Journal, **24**(2): 167–172. doi:10.1093/comjnl/24.2.167.

Watson, D.N. 1994. An implementation of natural neighbor interpolation. Dave Watson Publisher, Claremont, Australia.

List of symbols

$A^{(e)}$ element area
b opening value (m)
B bernoulli constant
$\mathbf{B}$ derivation of interpolation matrix
C_1 dirichlet boundary condition
C_2 neumann boundary condition
$C^{(e)}$ element boundary
d_1, d_2 conduit height at inbound and outbound section (m)
g acceleration due to gravity ($g = 9.806$ m/s^2)
$\mathbf{K}^{(e)}$ element system matrix
$\mathbf{K}$ total system matrix
m number of neighborhoods of any point
n unit normal from the free surface
N interpolation functions vector
p Pressure (mH$_2$O)
P total load vector
$P^{(e)}$ element load vector
Q the flow rate or discharge per unit width (m^3 s^{-1} m^{-1})
S problem domain
$S^{(e)}$ element domain
v, v_x, v_y velocity (m/s)
$\bar{v}$ free surface velocity (m/s)
V_0 import velocity (m/s)
V outlet velocity (m/s)
y the free surface elevation measured from an arbitrary datum (m)
Δy correction in y-direction (m)
ε prescribed accuracy
φ interpolation function
ψ the stream function (m^3 s^{-1} m^{-1})
$\boldsymbol{\psi}$ unknown nodal value vector

Appendix A. System matrix calculation

The number of neighborhoods for any point of a triangular element FEM is three whereas the number of neighborhoods in NEM can be more than three. If $a(x_1, y_1)$, $b(x_2, y_2)$, and $c(x_3, y_3)$ can be nodal coordinates of a triangular element, using eq. [22], matrix **B** can be evaluated as

$$[A1] \quad \mathbf{B} = \frac{1}{2A^{(e)}} \begin{bmatrix} y_2 - y_3 & y_3 - y_1 & y_1 - y_2 \\ x_3 - x_2 & x_1 - x_3 & x_2 - x_1 \end{bmatrix}$$

where $A^{(e)}$ is the element area. In the natural element method, it is necessary to use a suitable algorithm to find the shape functions and their derivatives to determine matrix **B**.

In FEM, the matrix **B** is constant over the triangular element, therefore with respect to Fig. A1, by using the nodal coordinates $(x_1, y_1) = (0, 0)$, $(x_2, y_2) = (2, 0.2)$, $(x_3, y_3) = (0.2, 2)$, $(x_4, y_4) = (2.2, 2.2)$ and using eq. [22] and eq. [A1], the system matrix for elements 1 and 2 can be obtained as

$$[A2] \quad \mathbf{K}^1 = \begin{bmatrix} 0.8182 & -0.4091 & -0.4091 \\ & 0.5101 & -0.1010 \\ \text{sym} & & 0.5101 \end{bmatrix}$$

$$[A3] \quad \mathbf{K}^2 = \begin{bmatrix} 0.5101 & -0.1010 & -0.4091 \\ & 0.5101 & -0.4091 \\ \text{sym} & & 0.8182 \end{bmatrix}$$

The assembled system matrix is

**Table A1.** Interpolation functions and their derivatives for different Gauss points.

	A_1	B_1	C_1	D_1	A_2	B_2	C_2	D_2
x	0.733	0.440	1.240	0.520	1.467	1.680	0.960	1.760
y	0.733	0.440	0.520	1.240	1.467	0.960	1.680	1.760
φ_1	0.375	0.601	0.258	0.258	0.042	0.058	0.058	0.001
$\partial\varphi_1/\partial x$	−0.340	−0.430	−0.373	−0.242	−0.114	−0.212	−0.081	−0.023
$\partial\varphi_1/\partial y$	−0.340	−0.430	−0.242	−0.373	−0.114	−0.081	−0.212	−0.023
φ_2	0.291	0.198	0.541	0.142	0.291	0.541	0.141	0.198
$\partial\varphi_2/\partial x$	0.391	0.481	0.423	0.292	0.164	0.262	0.131	0.074
$\partial\varphi_2/\partial y$	−0.164	−0.074	−0.262	−0.132	−0.390	−0.423	−0.292	−0.481
φ_3	0.291	0.198	0.141	0.542	0.291	0.141	0.541	0.198
$\partial\varphi_3/\partial x$	−0.164	−0.074	−0.132	−0.263	−0.390	−0.292	−0.423	−0.481
$\partial\varphi_3/\partial y$	0.391	0.481	0.297	0.423	0.164	0.131	0.262	0.074
φ_4	0.042	0.001	0.058	0.058	0.375	0.258	0.258	0.601
$\partial\varphi_4/\partial x$	0.114	0.023	0.081	0.212	0.340	0.242	0.373	0.431
$\partial\varphi_4/\partial y$	0.114	0.023	0.212	0.081	0.340	0.373	0.242	0.431

$$[A4] \quad \mathbf{K} = \begin{bmatrix} 0.8182 & -0.4091 & -0.4091 & 0 \\ & 1.0202 & -0.2020 & -0.4091 \\ & & 1.0202 & -0.409 \\ \text{sym} & & & 0.8182 \end{bmatrix}$$

In NEM, matrix **B** is not constant over the triangular element; therefore the system matrix can be obtained by using the Gauss integration method. The four-point Gauss integration method is used for $\mathbf{K}^1$ and $\mathbf{K}^2$ calculations. Therefore with respect to Fig. A1, by using eq. [22] and data presented in Table A1, the system matrix for the elements and the assembled system matrix are calculated as

$$[A5] \quad \mathbf{K}^1 = \begin{bmatrix} 0.533 & -0.215 & -0.215 & -0.103 \\ & 0.407 & -0.204 & 0.012 \\ & & 0.407 & 0.012 \\ \text{sym} & & & 0.097 \end{bmatrix}$$

$$[A6] \quad \mathbf{K}^2 = \begin{bmatrix} 0.079 & 0.012 & 0.012 & -0.103 \\ & 0.407 & -0.204 & -0.215 \\ & & 0.407 & -0.214 \\ \text{sym} & & & 0.533 \end{bmatrix}$$

Fig. A1. Delaunay triangulation of nodes and their Gauss points.
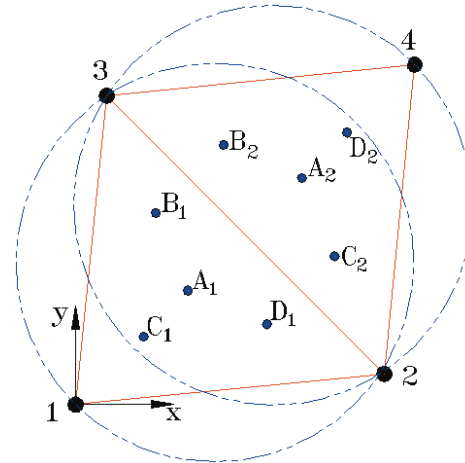
$$[A7] \quad \mathbf{K} = \begin{bmatrix} 0.619 & -0.203 & -0.203 & -0.206 \\ & 0.814 & -0.408 & -0.203 \\ & & 0.814 & -0.203 \\ \text{sym} & & & 0.612 \end{bmatrix}$$